NJC

Accepted Manuscript

This is an *Accepted Manuscript*, which has been through the Royal Society of Chemistry peer review process and has been accepted for publication.

Accepted Manuscripts are published online shortly after acceptance, before technical editing, formatting and proof reading. Using this free service, authors can make their results available to the community, in citable form, before we publish the edited article. We will replace this *Accepted Manuscript* with the edited and formatted *Advance Article* as soon as it is available.

You can find more information about *Accepted Manuscripts* in the Information for Authors.

Please note that technical editing may introduce minor changes to the text and/or graphics, which may alter content. The journal's standard Terms & Conditions and the Ethical guidelines still apply. In no event shall the Royal Society of Chemistry be held responsible for any errors or omissions in this *Accepted Manuscript* or any consequences arising from the use of any information it contains.

ROYAL SOCIETY OF CHEMISTRY

www.rsc.org/njc

Crystal structures, tunable emission and energy transfer of a novel $GdAl_{12}O_{18}N:Eu^{2+},Tb^{3+}$ oxynitrides phosphor

Wei Lü[a,*], Mengmeng Jiao [a,b], Jiansheng Huo [a,b], Baiqi Shao [a,b], Lingfei Zhao [a,b], Yang Feng [a,b] and Hongpeng You[a,*]

[a] State Key Laboratory of Rare Earth Resource Utilization, Changchun Institute of Applied Chemistry, Chinese Academy of Science, Changchun 130022, P. R. China.

[b] University of the Chinese Academy of Science, Beijing 100049,P. R. China.

*Corresponding author: E-mail address: hpyou@ciac.ac.cn; wlv@ciac.ac.cn.

Fax: +86-431-85698041; Tel: +86-431-85262798;

Abstract: We have synthesized a series of Eu^{2+} and Eu^{2+}/Tb^{3+} activated novel $GdAl_{12}O_{18}N$ oxynitrides phosphors by traditional solid state reaction. The crystal structural and photoluminescence properties of $GdAl_{12}O_{18}N:Eu^{2+}/Tb^{3+}$ phosphor are investigated. Rietveld structure refinement and photoluminescence properties of the obtained phosphor indicate that the $GdAl_{12}O_{18}N$ host has only one kind of Gd sites. $GdAl_{12}O_{18}N:Eu^{2+},Tb^{3+}$ samples exhibit a blue emission band peaking at 460 nm and a green line peaking at 550 nm, originating from the Eu^{2+} and Tb^{3+} ions, respectively. This energy transfer from Eu^{2+} to Tb^{3+} was confirmed by the decay times of energy donor Eu^{2+}. In addition, the mechanism of energy transfer from the Eu^{2+} to Tb^{3+} ions is demonstrated to be a dipole-quadrupole mechanism by the Inokuti-Hirayama (I-H) model. All results indicate that the Eu^{2+} and Tb^{3+} activated phosphor may be good candidates for blue-green components in UV white LEDs.

1. Introduction

The solid-state lighting sources based on white light emitting diodes (LEDs) has improved to overtake incandescent and fluorescent lighting types because of many advantages such as high brightness, ecofriendliness, long-life time, small size, low power consumption and fast response time.[1-5] At present, the combination of $Y_3Al_5O_{12}:Ce^{3+}$ (YAG:Ce) phosphor with blue InGaN chip is most frequently used. However, this method suffers the problems: white emitting color changes with input power and low color rendering index due to two-color mixing.[6-7] Another approach to obtain white light is the combination of UV or near-UV LEDs chips with tricolor (red, green and blue) phosphors.[8-27] WLEDs fabricated in this way can overcome the above problems and produce an excellent color rendering index and easily controll emission color properties. Therefore, researchers worldwide have investigated many other chemical compounds as suitable phosphors for solid-state lighting.

Nitride and oxynitride phosphors are newly developed members of the phosphor family, and have attracted many interests in recent years since they show good chemical and thermal stability. For example, the nitridosilicate activated by Eu^{2+} is likely to have a large crystal field splitting (CFS) and a low centroide level of 5d states of Eu^{2+} due to the coordination of N^{3-}having high covalency (nephelauxetic effect). Therefore, the excitation and emission stemming from Eu^{2+} tends to have a long wavelength, which is suitable for white LEDs. For this reason, nitridosilicate phosphors are currently being developed for white LEDs. Typical examples of developed nitridosilicate phosphors for white LEDs are $CaAlSiN_3:Eu$,[28] $La_3Si_6N_{11}:Ce$,[29,30] $(Ba,Sr,Ca)Si_2N_2O_2:Eu$,[31-32] $(Ba,Sr,Ca)_2Si_5N_8:Eu$,[33-36] $SrAlSi_4N_7:Eu$,[37] α-SiAlON,[38] and β-SiAlON.[39] Although a tremendous lot of work has been done on nitridosilicates and

nitridoaluminosilicates based materials, little attention has been paid to multinary (oxy)nitride systems based on aluminum.

In this study, we report the structure and luminescence properties of Eu^{2+}/Tb^{3+} activated $GdAl_{12}O_{18}N$ phosphors. The obtained samples have intense broad excitation band ranging from 250 nm to 410 nm which matches well with the popular UV LED chips. At the excitation of 365 nm, the $GdAl_{12}O_{18}N:Eu^{2+}$ can exhibit a blue emission band which extends from 400 to 600 nm. In Eu^{2+} and Tb^{3+} co-doped phosphor, a series of tunable blue-greenish colors can be obtained by varying the relative ratios of Eu^{2+}/Tb^{3+} in the irradiation of 330 nm. By utilizing the energy transfer between the Eu^{2+} and Tb^{3+} ions, we got intense blue-green phosphors which can be efficiently excited by UV LEDs. Moreover, the energy transfer mechanism between the Eu^{2+} and Tb^{3+} ions has been investigated systematically.

2. Experimental Section

A series of $Gd_{1-x-y}Al_{12}O_{18}N:xEu^{2+},yTb^{3+}$ phosphors were synthesized by conventional high temperature solid-state reaction. The starting materials Gd_2O_3 (99.99%), Al_2O_3 (A.R.), AlN (A.R.), Eu_2O_3 (99.99%), Tb_4O_7 (99.99%) were weighed in a proper stoichiometric ratio. After mixing and grinding in an agate mortar for 15 min, the mixture was placed in a crucible and then sintered at 1630 ºC for 4h in a reductive atmosphere (10% H_2 + 90% N_2). Finally, the prepared phosphors were cooled to room temperature and reground for further measurements.

The phase purity of all samples were identified by powder X-ray diffraction (XRD) analysis (Bruker AXS D8), with graphite monochromatized Cu Kα radiation (λ = 0.15405 nm) operating at 40 kV and 40 mA. The measurements of the photoluminescence (PL), photoluminescence excitation (PLE) were performed with a Hitachi F-7000 spectrometer equipped with a 150 W

xenon lamp as the excitation source. Crystal structure refinement employed the Rietveld method as implemented in the General Structure Analysis System (GSAS) program.[40] The luminescence decay curves were obtained from a Lecroy Wave Runner 6100 digital oscilloscope (1GHz) using a tunable laser (pulse width = 4 ns, gate = 50 ns) as the excitation source (Continuum Sunlite OPO).

3. Results and Discussion

3.1. Phase identification and crystal structure

All the prepared samples were characterized by the powder X-ray diffraction to verify their phase purity. Figure 1 demonstrates the typical powder XRD patterns of $Gd_{1-x}Al_{12}O_{18}N:xEu^{2+}$, and $Gd_{1-x-y}Al_{12}O_{18}N:0.04Eu^{2+},yTb^{3+}$ samples. They were found to be consistent with the standard data of $NdAl_{12}O_{18}N$ (JCPDS 42-1068),[41] indicating that our prepared samples are of phase purity and the doped ions do not cause any significant change.

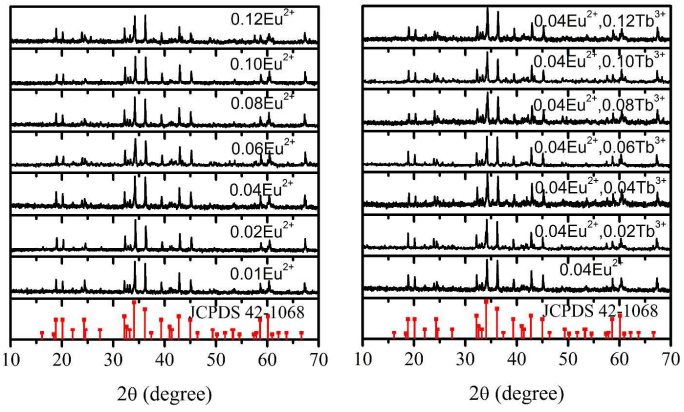

Figure 1. XRD patterns of typical prepared samples and standard data for $NdAl_{12}O_{18}N$ (JCPDS card no.42-1068).

In order to confirm the structure of the obtained samples, Rietveld structure refinement of $Gd_{0.96}Eu_{0.04}Al_{12}O_{18}N$ phosphor was performed using the powder diffraction data. Figure 2 depicts the results of Rietveld refinement pattern of the Eu^{2+} doped sample. In the refinement,

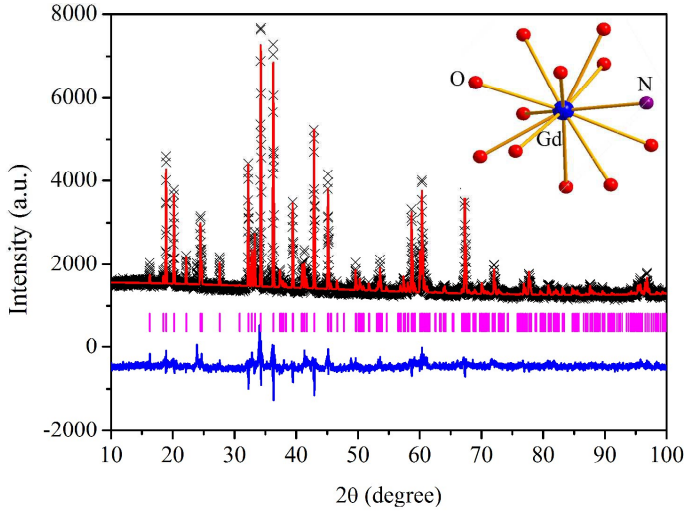

Figure 2. The experimental (crosses) and calculated (red solid line) powder XRD patterns of the $Gd_{0.96}Eu_{0.04}Al_{12}O_{18}N$ sample. The blue solid lines represent the difference between experimental and calculated data and the pink sticks mark the Bragg reflection positions. Inset: The coordination environment of the Gd^{3+} ions.

the previously reported crystallographic data of $CaAl_{12}O_9$(ICSD# 34394) which crystalizes in a hexagonal unit cell with the space group P63/MMC was employed as initial structure model. The refinement data χ^2 = 3.763, R_{wp} =5.03%, R_p = 3.56% indicate that all atom positions, fraction factors and temperature factors well satisfy the reflection condition. For $Gd_{0.96}Eu_{0.04}Al_{12}O_{18}N$ sample, the cell parameters were determined to be $a = b$ = 5.565068 Å, c = 21.875742 Å and V =586.69 $Å^3$. Figure 2 inset shows the unit cell structure of $Gd_{0.96}Al_{12}O_{18}N$:0.04Eu^{2+} sample together with the coordination environments of the Gd^{3+} sites. As far as we know, there is only one kinds of Ca^{2+} sites with 12-coordination in $CaAl_{12}O_9$ host.[42,43] In this case, the new sites are

assigned to Gd^{3+} replace Ca^{2+} ions and O^{2-} replace N^{3-} ions in their coordination. Therefore, our XRD refinement indicate that Gd^{3+} ions have only one 12-coordination numbers (CNs) as shown in Figure 2 inset. Basing on the effective ionic radii (r) of cations, it is demonstrated that Eu^{2+} (r = 1.25 Å) and Tb^{3+}(r = 1.04 Å) are expected to occupy the sites of Gd^{3+} (r = 1.05Å).

3.2. Luminescence properties of Eu^{2+}- doped materials

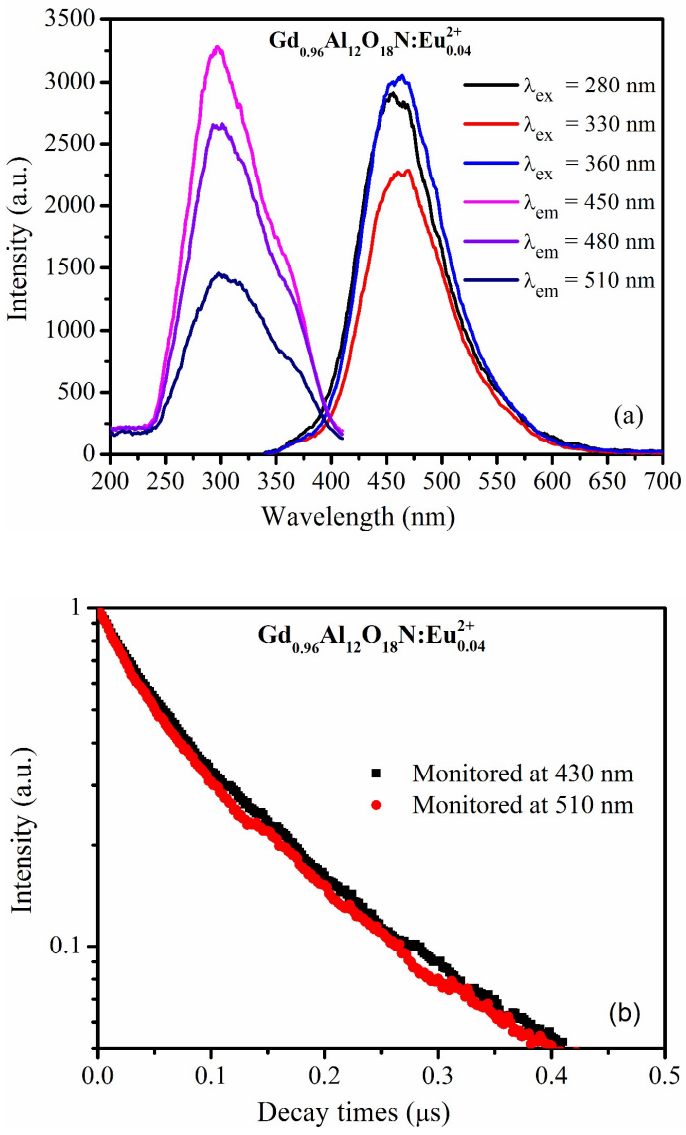

Figure 3. (a) PL and PLE spectra of $Gd_{0.96}Al_{12}O_{18}N:0.04Eu^{2+}$ phosphor. (b) Decay curves of $Gd_{0.96}Al_{12}O_{18}N:0.04Eu^{2+}$ phosphor monitored at different wavelengths.

Figure 3(a) depicts the PL and PLE spectra of the as-prepared $Gd_{0.96}Al_{12}O_{18}N:0.04Eu^{2+}$ phosphor. The sample shows a broad excitation band band from 250 to 400 nm with a maxium at 300 nm due to the $4f^7 \rightarrow 4f^6 5d^1$ transition of the Eu^{2+} ions. At the excitation of 330 nm, the PL spectrum shows an intense blue emission band attributed to the $4f^6 5d^1 \rightarrow 4f^7$ transition of the Eu^{2+} ion. With different excitation wavelengths of 280 and 360 nm, there are little changes in the blue emission except the emission intensity. This result indicates that Eu^{2+} ions substitute only one site in this system. Decay curves of $Gd_{0.96}Al_{12}O_{18}N:0.04Eu^{2+}$ are depicted in Fig. 3(b). When monitored at different wavelengths, the decay time of Eu^{2+} does not change, further supporting that Eu^{2+} ions substitute only one site. In order to investigate the effect of doping concentration on luminescence properites, a series of $Gd_{1-x}Al_{12}O_{18}N:xEu^{2+}$ (x = 0.02, 0.04, 0.06, 0.08, 0.10 and 0.12) phosphors were synthesized. Figure 4(a) shows the variation y of PL intensities of $Gd_{1-x}Al_{12}O_{18}N:xEu^{2+}$ with different doping contents. With an increasing Eu^{2+} doping concenration, the blue emission of the Eu^{2+} increases gradually and reaches a maximum at x = 0.06. For samples with Eu^{2+} dopant content higher than 0.06, concentration quenching is observed and the PL intensity is found to decrease with increasing Eu^{2+} dopant content. The critical distance R_C between Eu^{2+} ions can be estimated using the equation given by Blasse:[44]

$$R_C \approx 2\left[\frac{3V}{4\pi xN}\right]^{1/3} \qquad (1)$$

where V is the volume of the unit cell, N is the number of sites that lanthanide ion can occupy in per unit cell, and x is the critical concentration of doped ions. For the $GdAl_{12}O_{18}N$ host, N = 2, V=586.69 $Å^3$, and x is 6% for Eu^{2+}; therefore, the critical distance (R_C) was calculated to be

about 21.06 Å. Since the exchange interaction comes into effect only when the distance between activators is shorter than 5Å, the concentration quenching mechanism of the Eu^{2+} in the phosphor is dominated by the multipole-multipole interaction. According to Van Uiter's report, the emission intensity (I) per activator ion follows the equation:[45]

$$I / x = k\left[1 + b(x)^{q/3}\right]^{-1} \qquad (2)$$

Where x is the activator concentration, I/x is the emission intensity per activator concentration, k and β are constants for a given host in the same excitation condition, q = 6, 8 and 10 represent the dipole–dipole, dipole–quadrupole, and quadrupole–quadrupole interactions, respectively. By modifying the equation, log(I/x) acts a liner function of log(x) with a slop of (-q/3). To get the value of q, the relationship between log(I/x) and log(x) is plotted with x ranging from 0.06 to 0.12. From Figure 4(b), the q/3 is determined to be 1.62. Accordingly, q is calculated to be 4.86 which is close to 6. The result indicates that the concentration quenching mechanism of the Eu^{2+} emission in $Gd_{1-x}Al_{12}O_{18}N:xEu^{2+}$ host is dominated by the dipole-dipole interaction.

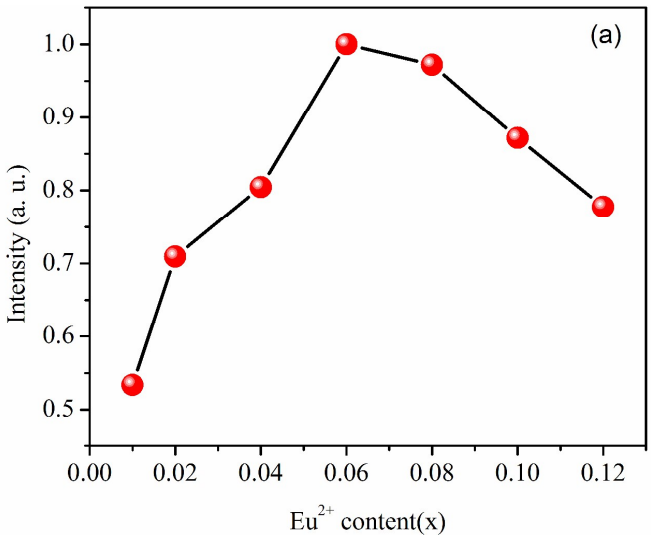

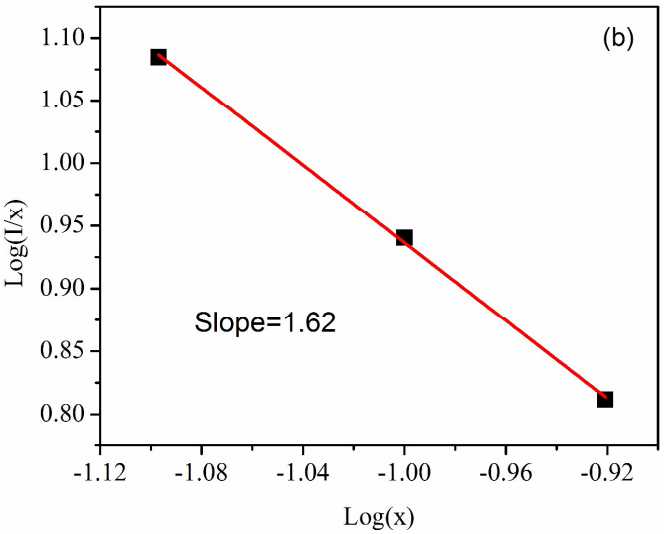

Figure 4. (a) The variation of emission intensity as a function of doped Eu^{2+} concentration. (b) Dependence of log(I/x) on log(x) in $Gd_{1-x}Al_{12}O_{18}N:xEu^{2+}$ phosphors.

3.3. Luminescence properties of $GdAl_{12}O_{18}N:Eu^{2+},Tb^{3+}$ phosphor and energy transfer between the Eu^{2+} and Tb^{3+} ions

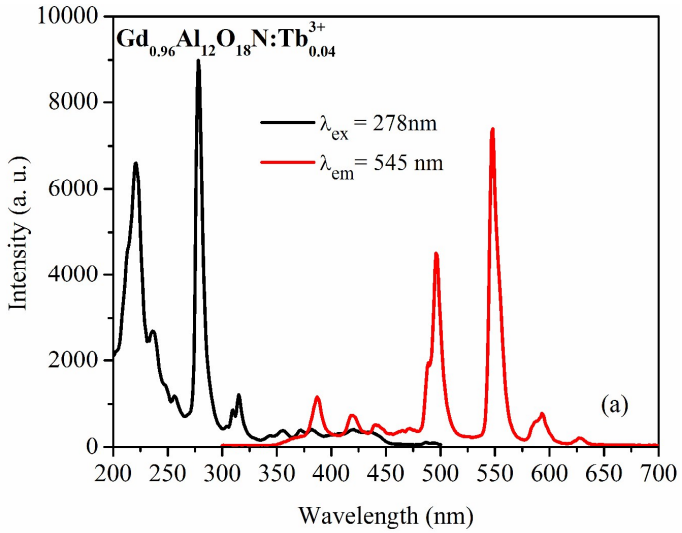

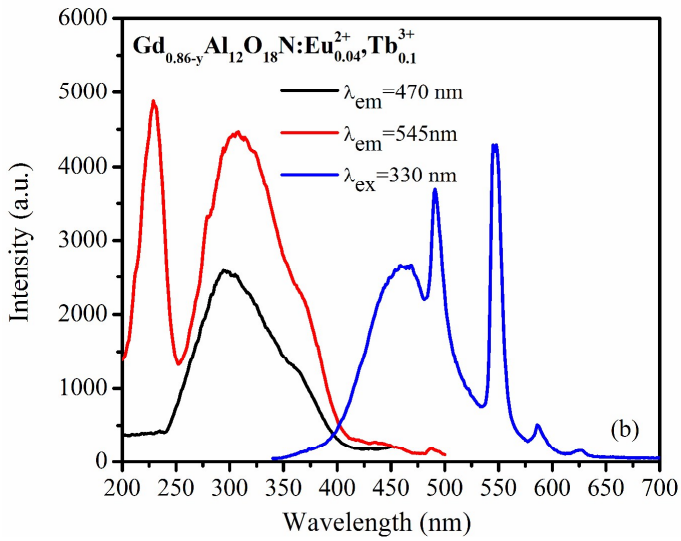

Figure 5. The PL and PLE spectra of (a) $Gd_{0.96}Al_{12}O_{18}N:0.04Tb^{3+}$ and (b) $Gd_{0.88}Al_{12}O_{18}N:0.04Eu^{2+},0.1Tb^{3+}$ phosphors.

Figure 5(a) illustrates the PL and PLE spectra of the $Gd_{0.96}Al_{12}O_{18}N:0.04Tb^{3+}$ phosphor. The PLE spectrum monitored at 545 nm exhibits a broad band and several weak peaks. The broad band from 200 to 250 nm centered at 230 nm is ascribed to the f-d transitions of the Tb^{3+} ions, while the excitation peaks at 275, 307 and 313 nm are originated from the transitions of $^8S_{7/2}\rightarrow{}^6I_{7/2}$, $^8S_{7/2}\rightarrow{}^6P_{5/2}$, and $^8S_{7/2}\rightarrow{}^6P_{7/2}$ of the Gd^{3+} ions. The peaks in the wavelength ranging from 280 to 500 nm are due to the intra-$4f^8$ transitions. At the excitation of 278 nm, the as-prepared $GdAl_{12}O_{18}N:0.04Tb^{3+}$ phosphor emits two sets of emissions. The emission peaks at 490, 543, 581, and 619 nm are assigned to the $^5D_4$-^7F_J (J=6,5,4,3) transitions, while the emission peaks at 380, 410, and 430 nm are due to the $^5D_3$-^7F_J transitions. Since there is an overlap between the PL spectra of $GdAl_{12}O_{18}N:Eu^{2+}$ and PLE spectra of $GdAl_{12}O_{18}N:Tb^{3+}$ phosphors, an effective energy transfer from the sensitizer Eu^{2+} to activator Tb^{3+} can be expected in the Eu^{2+} and Tb^{3+} co-doped phosphor. Figure 5(b) shows the PLE and PL spectra of the $Gd_{0.86}Al_{12}O_{18}N:0.04Eu^{2+},0.1Tb^{3+}$ phosphor. At the irradiation of 330 nm, the PL spectrum

exhibits both the Eu^{2+} and the typical Tb^{3+} emissions. Monitored at 545 nm which is the typical emission of the Tb^{3+} ions due to its $^5D_4$-$^7F_5$ transition, the phosphor shows absorption of both the Tb^{3+} and Eu^{2+} ions comparing with the PLE spectrum monitored at 470 nm. As seen from Figure 5b, the PLE spectrum is similar to that monitored at 545 nm. The above analysis on the PLE and PL spectra of the $Gd_{0.96-y}Al_{12}O_{18}N:0.04Eu^{2+},yTb^{3+}$ phosphor proves the occurrence of the energy transfer from the Eu^{2+} to Tb^{3+} ions.

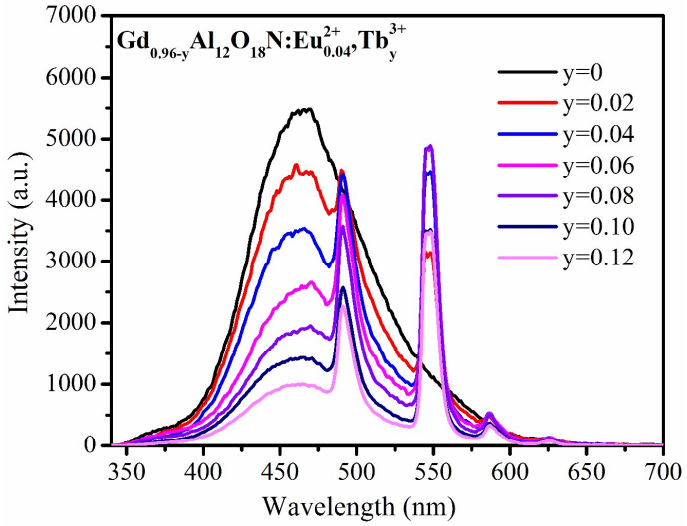

Figure 6. PL spectra of $Gd_{0.96-y}Al_{12}O_{18}N:0.04Eu^{2+},yTb^{3+}$ phosphor (y = 0, 0.02, 0.04, 0.06, 0.08, 0.1 and 0.12) under excitation wavelength of 330 nm.

Figure 6 shows the PL spectra of the $Gd_{0.96-y}Al_{12}O_{18}N:0.04Eu^{2+},yTb^{3+}$ (y = 0, 0.02, 0.04, 0.06, 0.08, 0.1 and 0.12) phosphors. With an increasing of the Tb^{3+} content, the emission intensity of the Eu^{2+} decreases monotonically. However, the intensity of the Tb^{3+} emission firstly increases to a maximum at $y = 0.08$, then decreases due to the concentration quenching.

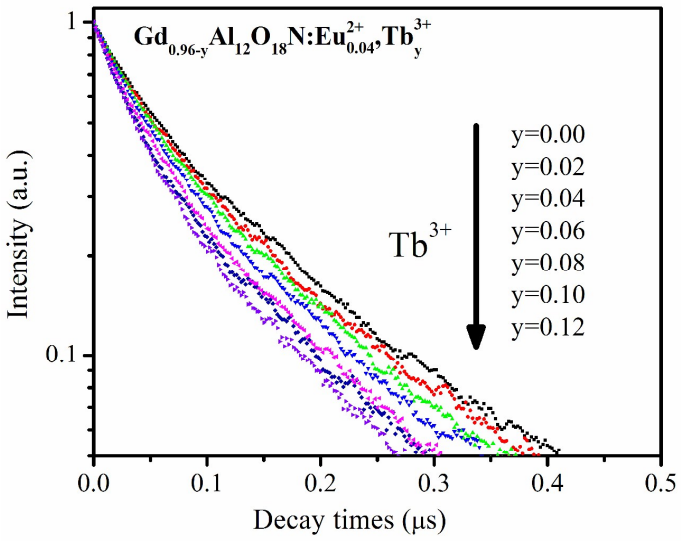

Figure 7. Decay curves for the luminescence of Eu^{2+} ions in $Gd_{0.96-y}Al_{12}O_{18}N:0.04Eu^{2+},yTb^{3+}$ samples. (excited at 330 nm, monitored at 470 nm)

To further study the energy transfer process, the fluorescence decay curves of the Eu^{2+} ions in $Gd_{0.96y}Al_{12}O_{18}N:0.04Eu^{2+},yTb^{3+}$ phosphors were measured by monitoring at 470 nm with an irradiation of 330 nm (Figure 7). In donor – acceptor energy transfer system, due to nonexponential decay of donor fluorescence intensity $I_D(t)$ in the presence of acceptors, we define an average fluorescence lifetime of the donors as [46,47]

$$\tau_D = \int_0^\infty I_D(t)dt, \qquad (3)$$

where $I_{D0}(t)$ is the decay function of donors in the absence of acceptors, which have normalized to its initial intensity. On the basis of equation (3), the lifetimes of the Eu^{2+} ions are determined to be 113, 106, 100, 95.1, 85.3, 79.9, and 74.0 ns for the $Gd_{0.96y}Al_{12}O_{18}N:0.04Eu^{2+},yTb^{3+}$ phosphors with y = 0, 0.02, 0.04, 0.06, 0.08, 0.1 and 0.12, respectively. Energy transfer efficiency

η_T between the Eu^{2+} and Tb^{3+} ions was also obtained from the decay lifetime by using the equation:

$$\eta_T = 1 - \frac{\tau}{\tau_0} \qquad (4)$$

where the τ and τ_0 are the lifetimes of sensitizer (Eu^{2+}) ion with and without the presence of activator (Tb^{3+}), respectively. The lifetimes and energy transfer efficiencies are plotted as a function of the Tb^{3+} concentration and shown in Figure 8. The average lifetimes decrease monotonously while the energy transfer efficiency increase gradually with the increment of the Tb^{3+} ions. The value of η_T reaches the maximum of 34.9% when y = 0.12, indicating that the energy transfer from the Eu^{2+} to Tb^{3+} is efficient.

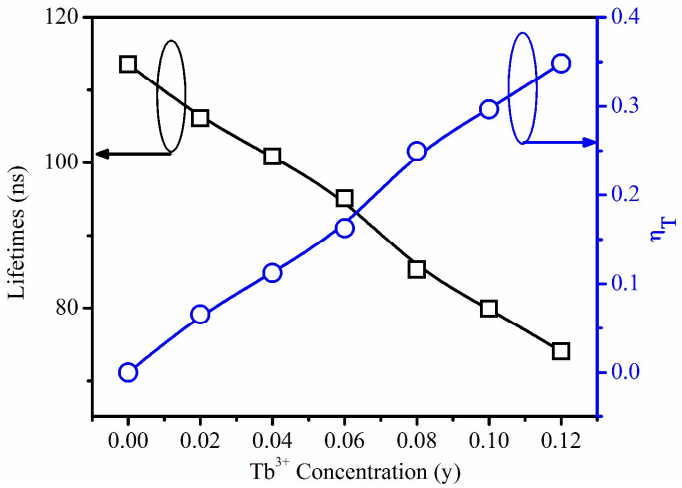

Figure 8. Dependence of the fluorescence lifetime of the Eu^{2+} and energy transfer efficiency on doped Tb^{3+} molar concentration in $Gd_{0.96-y}Al_{12}O_{18}N{:}0.04Eu^{2+},yTb^{3+}$ samples.

As described for the Eu^{2+} singly doped $GdAl_{12}O_{18}N$ part above, for this host, the R_c is calculated to be 17.76 Å using Eqn (1), where the value of X_c is defined as the critical concentration of dopant ions (total concentration of Eu^{2+} and Tb^{3+}, approximately 0.10), that is,

at which the luminescence intensity of Eu^{2+} is half of that in the sample without Tb^{3+}. According to Dexter's energy transfer expressions of multipolar interaction and Reisfeld's approximation, the following relation can be given as[48,49]

$$\frac{I_0}{I} \propto C^{n/3} \qquad (5)$$

where I_0 is the intrinsic luminescence intensity of the Eu^{2+} ions, I is the luminescence intensity of the Eu^{2+} ions with the activator (Tb^{3+}) present, and C is the doping concentration of the Tb^{3+} ions. The plots of (I_0/I) versus $C^{n/3}$ with n= 6, 8, and 10 correspond to dipole-dipole, dipole-quadrupole and quadrupole-quadrupole interactions. Figure 9 illustrates the relationships between (I_0/I) versus $C^{n/3}$, and a liner relation is observed when n = 8. This result clearly indicates that the energy transfer mechanism from the Eu^{2+} to Tb^{3+} ions is a dipole-quadrupole reaction.

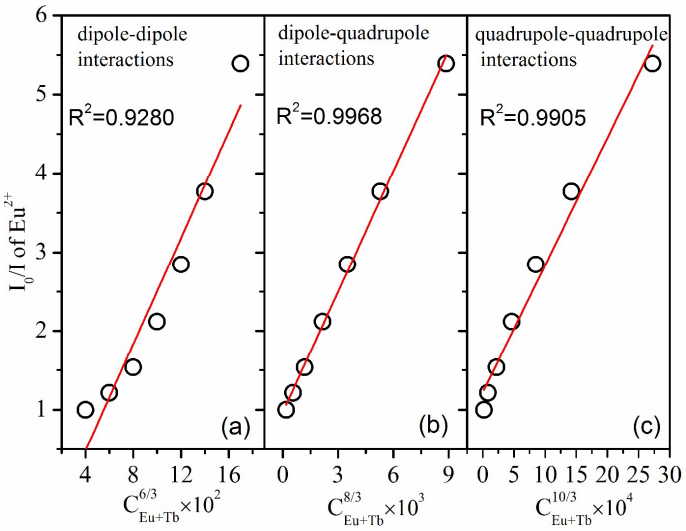

Figure 9. Experimental data plots of $\log\{\ln[I_{D0}(t)/I_D(t)]\}$ versus $\log(t)$ of Eu^{2+} in $Gd_{0.96-y}Al_{12}O_{18}N$:0.04$Eu^{2+}$,y$Tb^{3+}$ samples. The red lines indicate the fitting behaviors.

The energy transfer critical distance (Rc) between Eu^{2+} and Tb^{3+} ions can also be obtained through the spectral overlap method, which can be expressed by the following equation [50,51]

$$R_C^8 = 3.024\times10^{12}\,\lambda_S^2 f_q \int \frac{F_S(E)F_A(E)dE}{E^4} \qquad (6)$$

where f_d is the oscillator strength of the involved absorption transition of the acceptor. It is a pity that the oscillator strength of the Tb^{3+} quadrupole transition (f_q) did not obtain up to now. However, it was suggested by Verstegen et al. that the ratio f_q/f_d is about 10^{-3}-10^{-2}, where f_d = 10^{-6} is the oscillator strength of the electric dipole transitions. λ_S = 4630 Å is the wavelength of the strongest intensity of Eu^{2+}; E is the energy involved in the transfer (in eV), and $\int F_S(E)F_A(E)/E^4dE$ represents the spectral overlap between the normalized shapes of the Ce^{3+} emission $F_S(E)$ and the Tb^{3+} excitation $F_A(E)$, and in our case it is calculated to be about $0.009692eV^{-5}$. Accordingly, the R_c value is calculated to be 12.58–16.78 Å, which agrees approximately with that obtained by using the concentration quenching method (17.76Å).

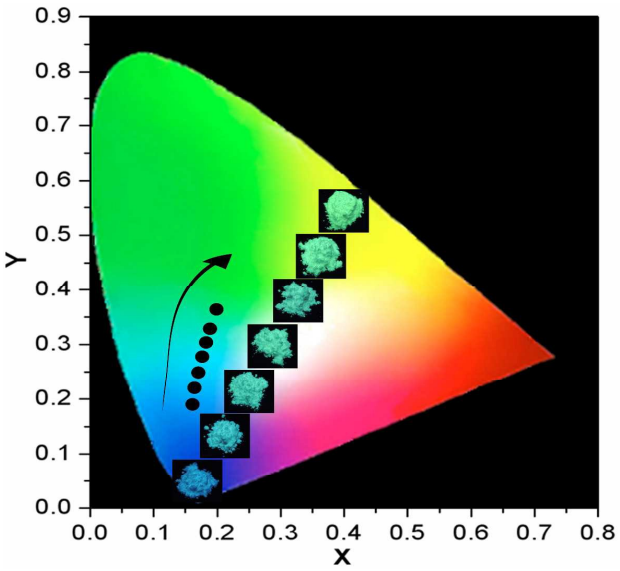

Figure 10. CIE chromaticity diagram for $Gd_{0.96-y}Al_{12}O_{18}N$:$0.04Eu^{2+}$,$yTb^{3+}$ phosphors, together with their corresponding photographs under a 365 nm UV lamp.

Figure 10 shows the Commission International de L'Eclairage (CIE) chromaticity diagram for several typical $Gd_{0.96-y}Al_{12}O_{18}N:0.04Eu^{2+},yTb^{3+}$ samples, together with their corresponding photographs. It can be seen that the emitting colors of the phosphors can be easily modulated from blue to green by simply varying the value of *y* from 0 to 0.12. Accordingly, the corresponding CIE coordinates of $Gd_{0.96-y}Al_{12}O_{18}N:0.04Eu^{2+},yTb^{3+}$ change from (0.160, 0.196) to (0.209, 0.345), due to the different emission composition of the Eu^{2+} and Tb^{3+} ions. Thus, blue-green emitting phosphors which can be efficiently excited by the UV chips are obtained via the energy transfer from the Eu^{2+} to Tb^{3+} ions. The $Gd_{0.96-y}Al_{12}O_{18}N:0.04Eu^{2+},yTb^{3+}$ phosphor may have potential value as blue-greenish phosphors used for UV white LEDs.

4. Conclusions

In summary, a series of Eu^{2+}/Tb^{3+} activated $GdAl_{12}O_{18}N$ phosphors had been synthesized and investigated for the first time. The $GdAl_{12}O_{18}N$ host has a hexagonal unit cell with cell parameters $a = b = 5.565068$ Å, $c = 21.875742$ Å and $V = 586.69$ Å^3, and $Z = 2$. The obtained phosphors have a broad excitation band ranging from 250 to 400 nm which can match perfectly with the commercial UV LED chips. At the excitation of 365 nm, the $Gd_{0.96}Al_{12}O_{18}N:0.04Eu^{2+}$ phosphors can emit intense blue light with an optimal concentration of the Eu^{2+} being 0.06. The critical distance for the Eu^{2+} has been calculated to be 21.06 Å and the concentration quenching is dominated by dipole-dipole interaction. For the co-doped samples, tunable colors from blue to green can be realized by singly varying the doping concentration of the Tb^{3+} ion at the irradiation of 365 nm. The dipole-quadrupole interaction mechanism should be mainly responsible for the energy transfer from the Eu^{2+} to Tb^{3+} ions. The experimental results indicate that the $Gd_{0.96-y}Al_{12}O_{18}N:0.04Eu^{2+},yTb^{3+}$ phosphor may have promising application in UV white LEDs.

Acknowledgements

This work is financially supported by the National Natural Science Foundation of China (Grant Nos. 11304309 and 51472236) and the National Basic Research Program of China (973 Program, Grant no 2014CB643803), and the Fund for Creative Research Groups (Grant No. 21221061).

Reference

1 C. Feldmann, T. Jüstel, C. R. Ronda and P. J. Schmidt, *Adv. Funct. Mater.,* 2003, **13**, 511.

2 R. J. Xie, N. Hirosaki, T. Suehiro, F. F. Xu and M. Mitomo, *Chem. Mater.,* 2006, **18**, 5518.

3 J. H. Oh, S. J. Yang and Y. R. Do, *Light:Sci. Appl.* 2014, **3**, e141.

4 G. G. Li, Y. Tian, Y. Zhao and J. Lin, *Chem. Soc. Rev.*, 2015, **44**, 8688.

5 M. M. Shang, C. X. Li and J. Lin, *Chem. Soc. Rev.*, 2014, **43**, 1372.

6 Z. D. Hao, J. H. Zhang, X. Zhang, X. Y. Sun, Y. S. Luo, S. Z. Lu and X. J. Wang, *Appl. Phys. Lett.,* 2007, **90(26)**, 261113.

7 J. S. Kim, P. E. Jeon, Y. H. Park, J. C. Choi, H. L. Park, G. C. Kim and T. W Kim, *Appl. Phys. Lett.*, 2004, **85(17)**, 3696.

8 X. F. Li, J. D. Budai, F. Liu, J. Y. Howe, J. H. Zhang, X. J. Wang, Z. J. Gu, C. J. Sun, R.S. Meltzer and Z. W. Pan, *Light:Sci. Appl.* 2013, **2**, e50.

9 W. J. Yang and T. M. Chen, *Appl. Phys. Lett.,* 2007, **90(17)**, 171908.

10 W. Lü, Z. D. Hao, X. Zhang, Y. S. Luo, X. J. Wang and J. H. Zhang, *Inorg. Chem.*, 2011, **50**, 7846.

11 G. G. Li, D. L. Geng, M. M. Shang, D. M. Yang, Y. Zhang, C. Peng, Z. Y. Cheng and J. Lin, *J. Phys. Chem. C.*, 2011, **115(44)**, 21882.

12 M. M. Shang, D. L. Geng, Y. Zhang, G. G. Li, D. M. Yang, X. J. Kang and J. Lin, *J. Mater. Chem.,* 2012, **22**, 19094.

13 W. Lü, N. Guo, Y. C. Jia, Q. Zhao, W. Z. Lv, M. M. Jiao, B. Q. Shao and H. P. You, *Inorg. Chem.*, 2013, **52**, 3007.

14 Z. Y. Mao, Y. C. Zhu, L. Gan, Y. Zeng, F. F. Xu, Y. Wang, H. Tian, J. Li and D. J. Wang, *J. Lumin.*, 2013, **134**, 148.

15 M. A. Mickens and Z. Assefa, *J. Lumin.*, 2014, **145**, 498.

16 W. Lü, Y. C. Jia, W. Z. Lv, Q. Zhao and H. P. You, *Chem. Commun.,* 2014, **50**, 2635.

17 K. Li, D. L. Geng, M. M. Shang, Y. Zhang, H. Z. Lian and J. Lin,*J. Phys. Chem. C.*, 2014, **118**, 11026.

18 X. G. Zhang and M. L. Gong,*Dalton Trans.*, 2014, **43**, 2465.

19 X. Chen, P. P. Dai, X. T. Zhang, C. Li, S. Lu, X. L. Wang, Y. Jia and Y. C. Liu, *Inorg. Chem.*, 2014, **53**, 3441.

20 H. K. Liu, Y. Luo, Z. Y. Mao, L. B. Liao and Z. G. Xia,*J. Mater. Chem. C*, 2014, **2**, 1619.

21 W. Lü, W. Z. Lv, Q. Zhao, M. M. Jiao, B. Q. Shao and H. P. You, *J. Mater. Chem. C*, 2015, **3**, 2334.

22 L, Bian, C.W. Liu, J. Gao and X. P. Jing, *RSC Adv.,* 2015, **5**, 69458.

23 S. Miao, Z. Xia, M. S. Molokeev, J. Zhang and Q. Liu, *J. Mater. Chem. C*, 2015, **3**, 8322.

24 Q. Bai, Z. Wang, P. Li, S. Xu, T. Li and Z. Yang, NewJ.Chem., 2015, **39**, 8933.

25 N. Komuro, M. Mikami, Y. Shimomura, E. G. Bithellc and A. K. Cheethamd, J. Mater. Chem. C, 2015, **3**, 204.

26 C. Liang, H. You, Y. Fu, X. Teng, K. Liu and J. He, Dalton Trans., 2015, **44**, 8100.

27 B. Zhang, H. Zhong, C. Cai, L.Y. Hao, X. Xu, S. Agathopoulos, L and J. Yin, Mater. Res. Bull., 2015, **72**, 83.

28 Y. Q. Li, N. Hirosaki, R.-J. Xie, T. Takeda and M. Mitomo, *Chem. Mater.*, 2008, **20**, 6704.

29 T. Seto, N. Kijima and N. Hirosaki, *ECS Trans.*, 2009, **25**, 247.

30 T. Suehiro, N. Hirosaki and R.-J. Xie, *ACS Appl. Mater. Interfaces*, 2011, **3**, 811.

31 V. Bachmann, T. Jüstel, A. Meijerink, C. Ronda and P. J. Schmidt, *J. Lumin.*, 2006, **121**, 441.

32 V. Bachmann, C. Ronda, O. Oeckler, W. Schnick and A. Meijerink, *Chem. Mater.*, 2009, **21**, 316.

33 G. Li, C. C. Lin, W. T. Chen, M. S. Molokeev, V. V. Atuchin, C. Y. Chiang, W. Zhou, C. W. Wang, W. H. Li, H. S. Sheu, T. S. Chan, C. Ma and R. S. Liu, *Chem. Mater.*, 2014, **26**, 2991.

34 R.-J. Xie, N. Hirosaki, T. Suehiro, F.-F. Xu and M. Mitomo, *Chem. Mater.*, 2006, **18**, 5578.

35 Y. Q. Li, J. E. J. van Steen, J. W. H. van Krevel, G. Botty, A. C. A. Delsing, F. J. DiSalvo, G. de With and H. T. Hintzen, *J. Alloys Compd.*, 2006, **417**, 273.

36 X. Piao, T.Horikawa, H. Hanzawa and K. Machida, *Appl. Phys. Lett.*, 2006, **88**, 161908.

37 L. Zhang, J. Zhang, X. Zhang, Z. Hao, H. Zhao and Y. Luo, *ACS Appl. Mater. Interfaces*, 2013, **5**, 12839.

38 N. Hirosaki, R.-J. Xie, K. Kimoto, T. Sekiguchi, Y. Yamamoto, T. Suehiro and M. Mitomo, *Appl. Phys. Lett.*, 2005, **86**, 211905.

39 R.-J. Xie, N. Hirosaki, M. Mitomo, Y. Yamamoto, T. Suehiro and N. Ohashi, *J. Am. Ceram. Soc.*, 2004, **87**, 1308.

40 C. Larson and R. B. Von Dreele, General Structure Analysis System (GSAS), Los Alamos National Laboratory, Los Alamos, NM, 1994, pp. 86–748.

41 W. Y. Sun and T. S. Yen, *Mater. Lett.*, 1989, **8**, 145.

42 N. Iyi, Z. Inoue, S. Takekawa and S. Kimura, *J. Solid State Chem.*, 1984, **52**, 66.

43 G. Costa, M. J. Ribeiro, W. Haijiaji, M. P. Seahra, J. A. Labrincha, M. Dondi and G. Cruciani, *J. Eur. Ceram. Soc.*, 2009, **29**, 2671.

44 G. Blasse, *Philips Res. Rep.*, 1969, **24**, 131.

45 L. G. Van Uitert, *J. Electrochem. Soc.*, 1967, **114**, 1048.

46 L. Wang, X. Zhang, Z. D. Hao, Y. S. Luo, J. H. Zhang and X. J. Wang, *J. Appl. Phys.*, 2010, **108**, 093515.

47 J. H. Zhang, Z. D. Hao, J. Li, X. Zhang, Y. S. Luo and G. H. Pan, *Light:Sci. Appl.*, 2015, **4**, e239.

48 C. C. Lin, R. S. Liu, Y. S. Tang and S. F. Hu, *J. Electrochem. Soc.*, 2008, **155**, J248.

49 D. L. Dexter and D. L. Dexter, *J. Chem. Phys.*, 1953, **21**, 836.

50 D. L. Dexter and J. A. Schulman, *J. Chem. Phys.*, 1954, **22**, 1063.

51 J. M. P. J. Verstegen, J. L. Sommerdijk and J. G. Verriet, *J. Lumin.*, 1973, **6**, 425.

Table of Content

Crystal structures, tunable emission and energy transfer of a novel $GdAl_{12}O_{18}N:Eu^{2+},Tb^{3+}$ oxynitrides phosphor

Wei Lü[a,*], Mengmeng Jiao [a,b], Jiansheng Huo [a,b], Baiqi Shao [a,b], Lingfei Zhao [a,b], Yang Feng [a,b] and Hongpeng You[a,*]

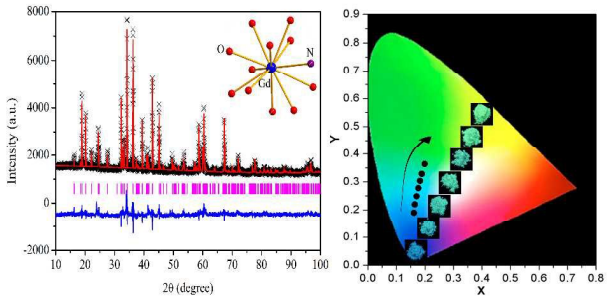

By tuning the relative content of the doped ions, tunable blue-green emission can be obtained by the irradiation at 365 nm.